Tidal surface states as fingerprints of non-Hermitian nodal knot metals

Ching Hua Lee,* Guangjie Li, Yuhan Liu, Tommy Tai, Ronny Thomale,† and Xiao Zhang‡

SUPPLEMENTARY INFORMATION

SUPPLEMENTARY NOTE 1

In this section, we provide a more detailed analysis of the complex spectral properties i.e. imaginary gap and vorticity of the two models most featured in the main text, namely the Hopf-link and Trefoil nodal knot metals (NKMs).

Hopf-Link NKM

We analyze the tidal region of the simplest nodal knot metal (NKM) - the non-Hermitian Hopf-link. In Figs. 2a,b of the main text, the analytically derived topological tidal region from Eq. 1 of the main text Fig. 2(a) agrees exactly with the trenches (band intersections) in the imaginary band structure plot Fig. 2(b), which define a tidal island. Note that other auxiliary peaks within the island, which possibly connect with other bands, play no role in topology.

As a further elaboration of the marine landscape analogy, consider the periodic boundary conditions (PBC) scenario governed by Bloch states represented by the $\beta = \log|z| = 0$ sea level, i.e. real $k_\perp = -i\log z$. As the boundary couplings are gradually switched off, a spectral flow ensues [1], corresponding to a shift in the tidal (sea) level. The spectral flow stops at the trenches, which demarcate the "actual tidal" boundary of the topological region.

This spectral flow is laid out in detail in the figures that follow, Figs. S1,S2,S3, which feature the spectra at various representative surface momenta for each of the three possible surface terminations, $\hat{e}_1, \hat{e}_2, \hat{e}_3$ respectively. Since $h_z(\mathbf{k}) = 0$ for all $\mathbf{k}$, topological boundary modes, if any, reside at the origin. Note that, due to limitations of numerical convergence, the numerical OBC (in black) spectra (under open boundary conditions) sometimes do not converge onto lines, even though they rigorously should in the OBC limit of exactly zero boundary hoppings. This illustrates that, under the skin effect, even infinitesimally small noise can significantly affect the spectrum.

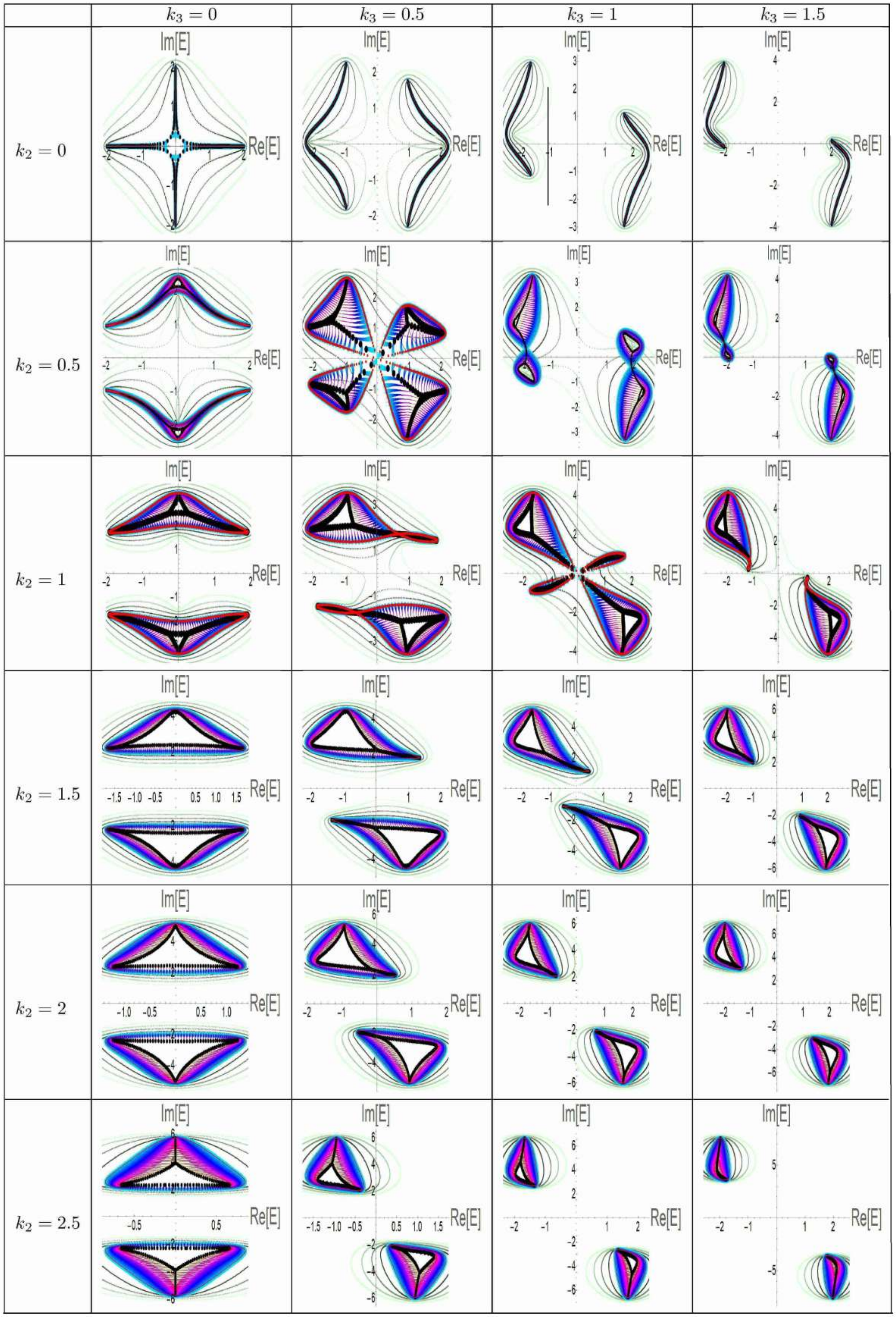

Supplemental Figure S1: Complex spectra of the non-Hermitian Hopf nodal knot metal (NKM) with $\hat{e}_1$ surface termination. Blue-magenta curves denote the spectral flow between the spectra under periodic boundary conditions (red) and open boundary conditions (black). Background contours denote level curves of constant $\log |z|$ where $z = e^{ik_1}$.

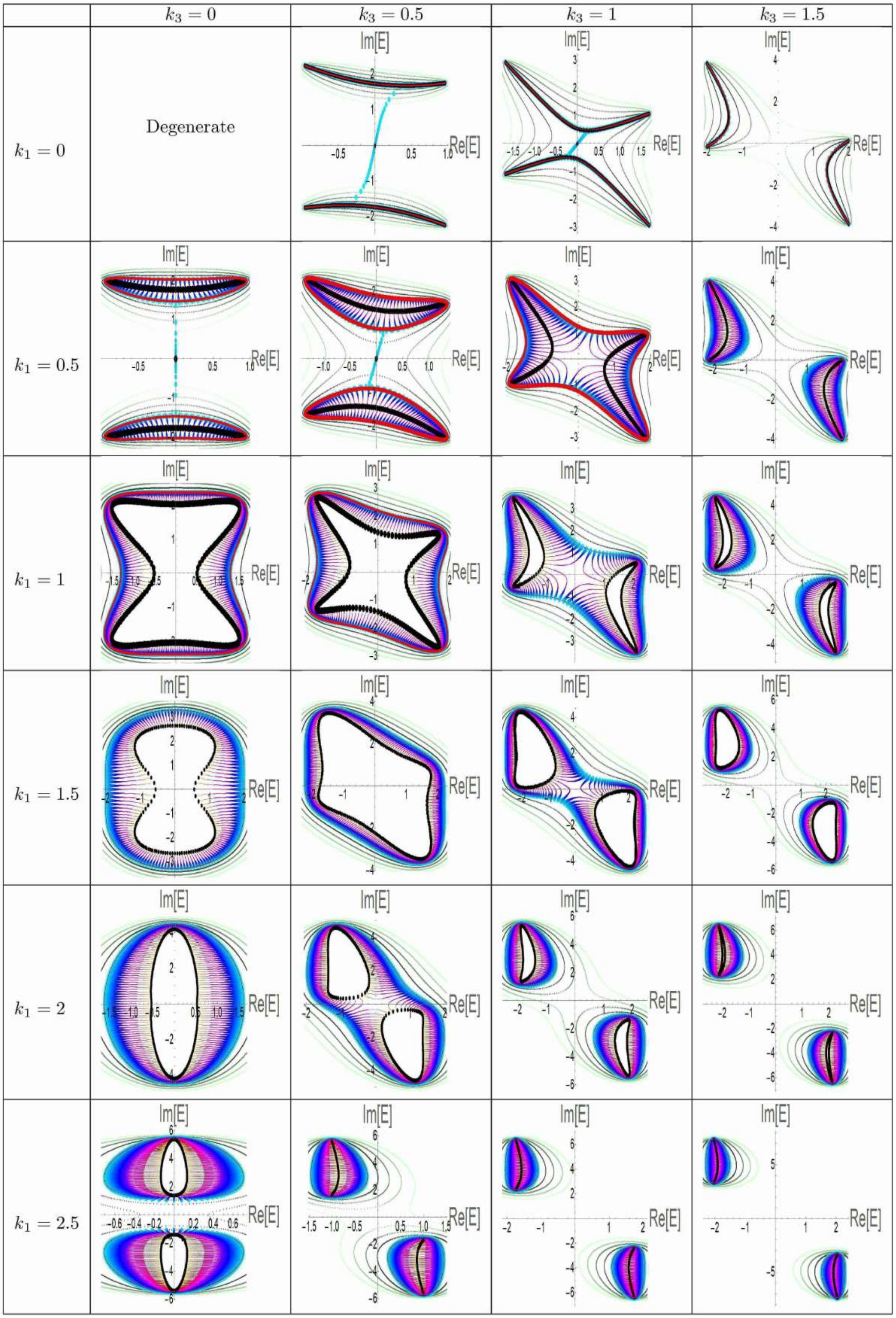

Supplemental Figure S2: Complex spectra of the non-Hermitian Hopf nodal knot metal (NKM) with $\hat{e}_2$ surface termination. Blue-magenta curves denote the spectral flow between the spectra under periodic boundary conditions (red) and open boundary conditions (black). Background contours denote level curves of constant $\log|z|$ where $z = e^{ik_2}$.

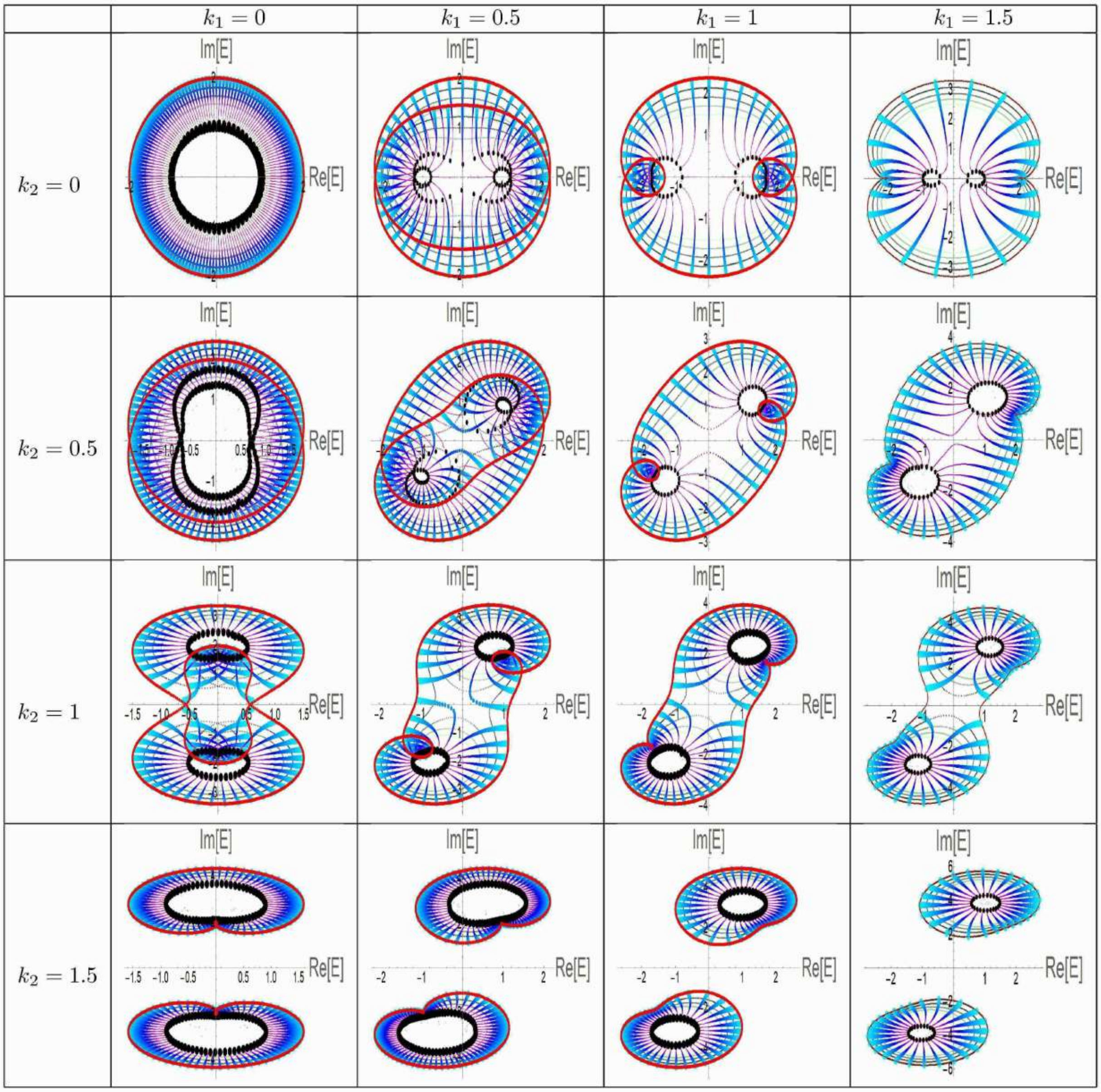

Supplemental Figure S3: Complex spectra of the non-Hermitian Hopf nodal knot metal (NKM) with $\hat{e}_3$ surface termination. Blue-magenta curves denote the spectral flow between the spectra under periodic boundary conditions (red) and open boundary conditions (black). Background contours denote level curves of constant $\log |z|$ where $z = e^{ik_3}$. Black circles represent the skin boundary states obtained at maximal numerical convergence; note the lack of well-defined curves of skin states.

Trefoil NKM

Here we provide further details of the complex analytic properties of our non-Hermitian Trefoil NKM model.

Compared to the Hopf-link, the Trefoil NKM has a much richer complex gap band structure, with 8 solutions (bands). As explained and shown in Fig. 2(c-d) in the main text, only the intersection between the 4th and the 5th bands are of topological significance. Even so, there exist subtleties on the types of intersections that are actually significant. As explained in the main text, and present for the full surface Brillouin Zones (BZs) below, topological boundaries correspond only to the boundaries between the light and dark colored region in the plots of Fig. S4 below. The other intersections, i.e. between light red and blue regions, also correspond to trenches, but not the tidal trenches of topological significance.

Also presented in the following figures (Figs. S5,S6,S7) are the spectral flow plots, which are somewhat more intricate than those of the non-Hermitian Hopf model. Since $h_z(\mathbf{k}) = i\gamma$ with γ set to unity, topological boundary modes, if any, occur at $\pm i$. Like in the Hopf-link case, limitations of numerical tolerance give rise to infinitesimally small noise in the boundary hoppings, which cause some OBC spectra (black) not to converge fully onto curves or straight lines.

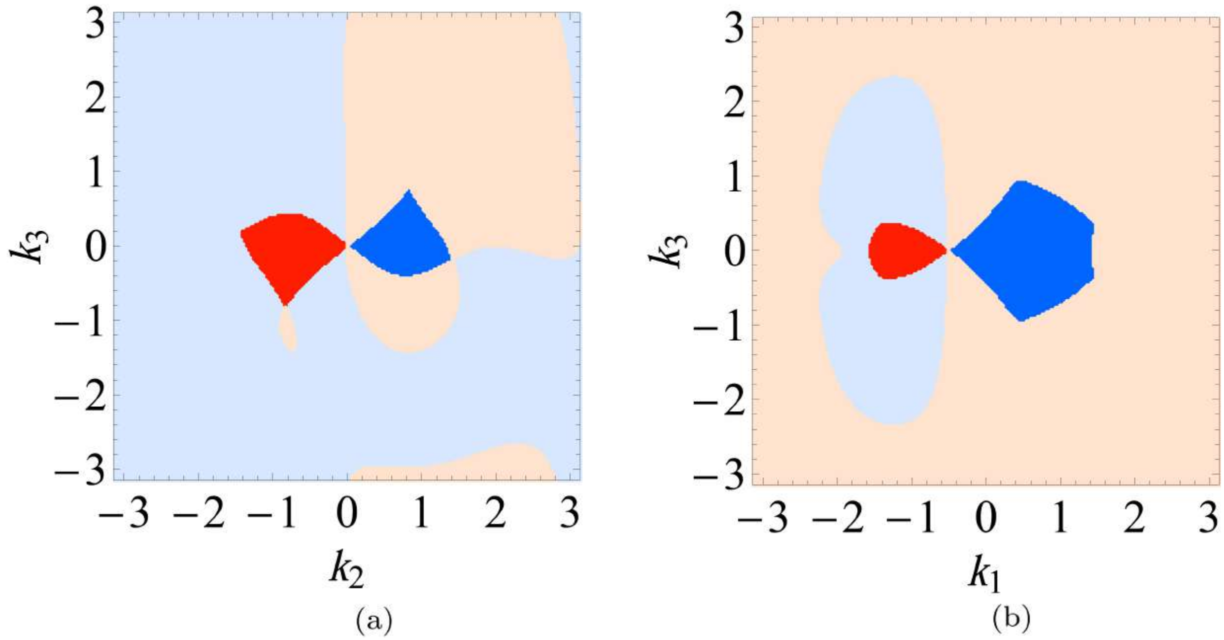

Supplemental Figure S4: Plots of the 4-th and 5-th $\log|z|$ (where $z = e^{ik_j}$, j=1,2,3) bands like in Fig. 2b of the main text, for the non-Hermitian Trefoil knot nodal knot metal with a) $\hat{e}_1$ and b) $\hat{e}_2$ surface terminations.

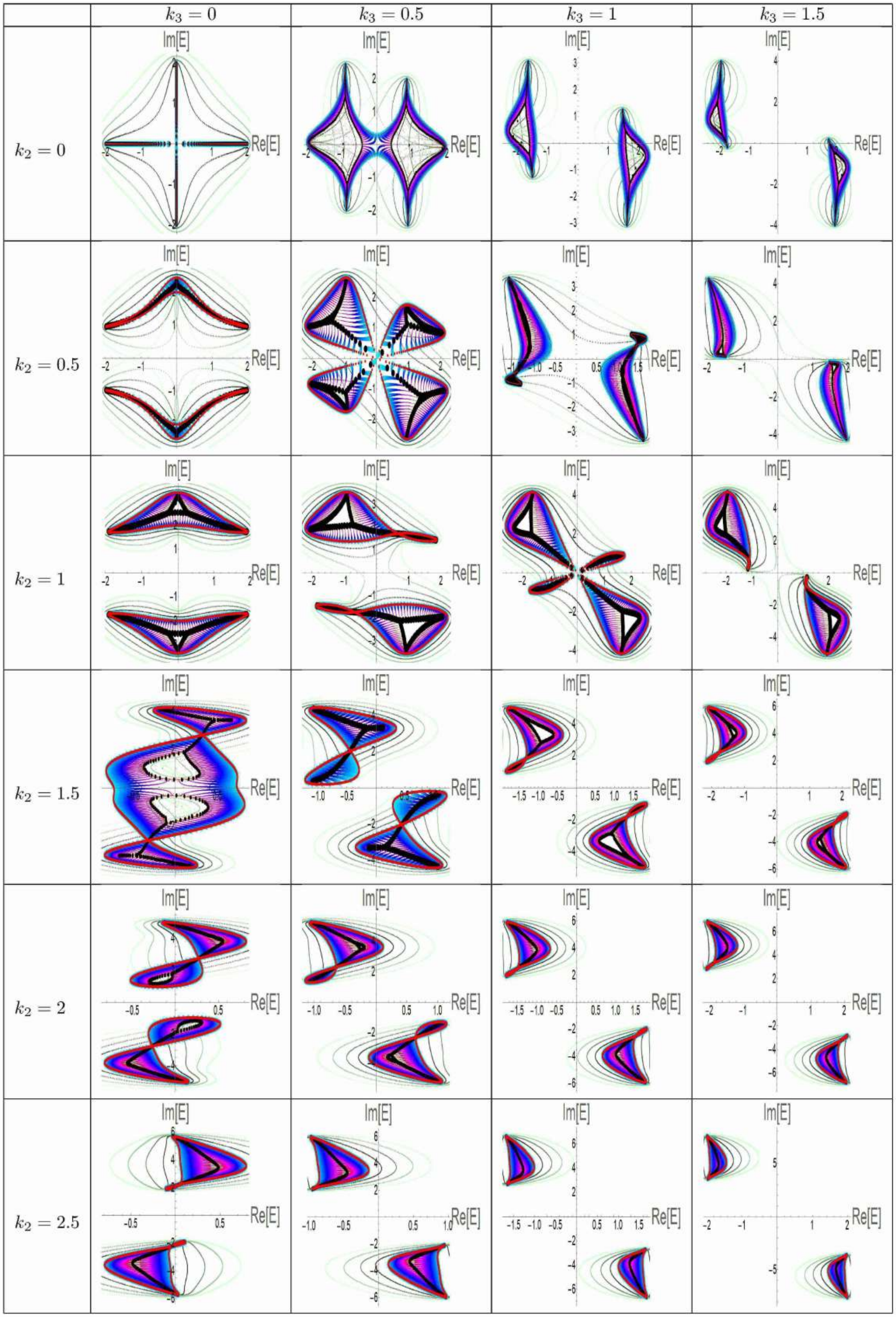

Supplemental Figure S5: Complex spectra of the non-Hermitian Trefoil nodal knot metal (NKM) with $\hat{e}_1$ surface termination. Blue-magenta curves denote the spectral flow between the spectra under periodic boundary conditions (red) and open boundary conditions (black). Background contours denote level curves of constant $\log |z|$ where $z = e^{ik_1}$.

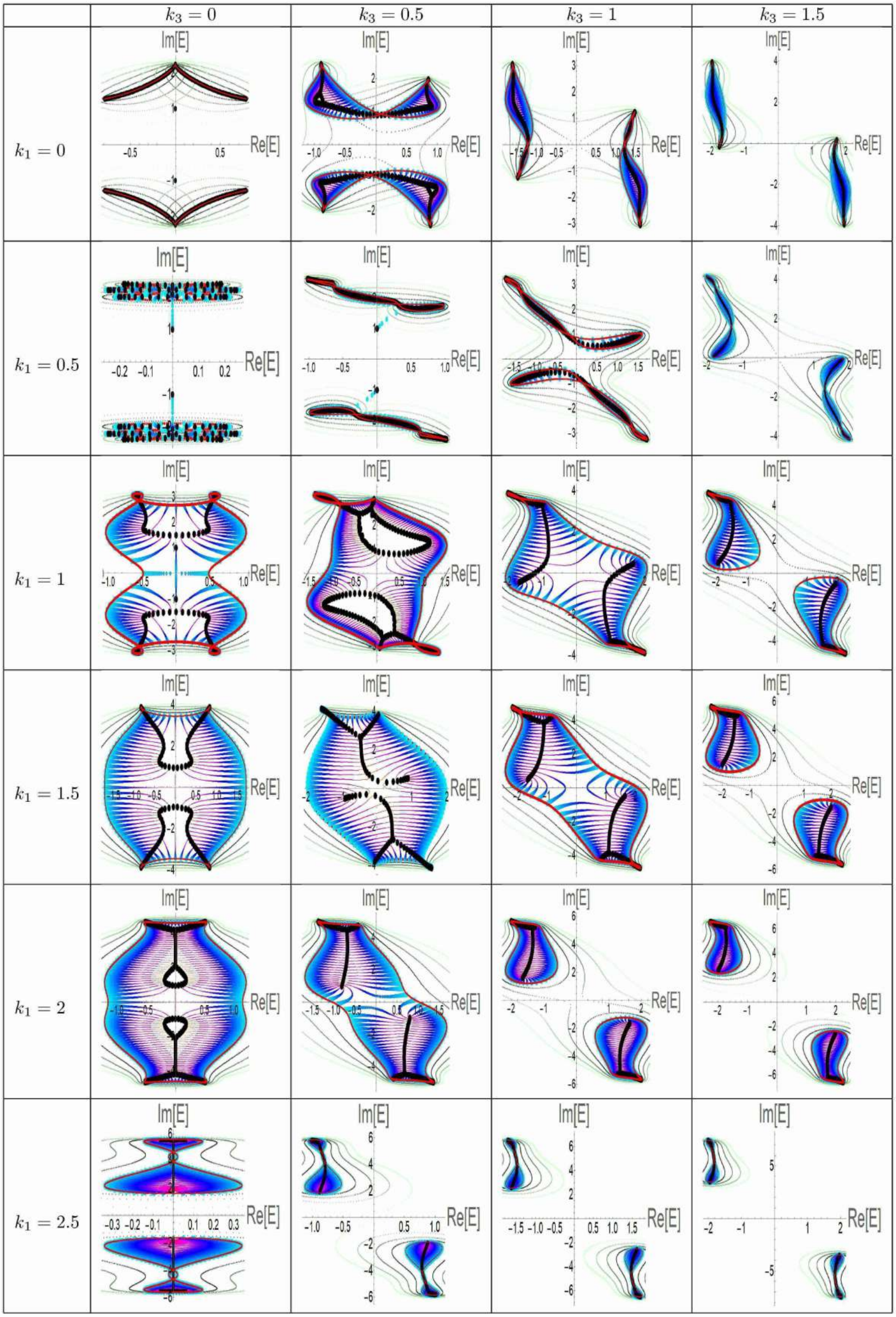

Supplemental Figure S6: Complex spectra of the non-Hermitian Trefoil nodal knot metal (NKM) with $\hat{e}_2$ surface termination. Blue-magenta curves denote the spectral flow between the spectra under periodic boundary conditions (red) and open boundary conditions (black). Background contours denote level curves of constant $\log |z|$ where $z = e^{ik_2}$.

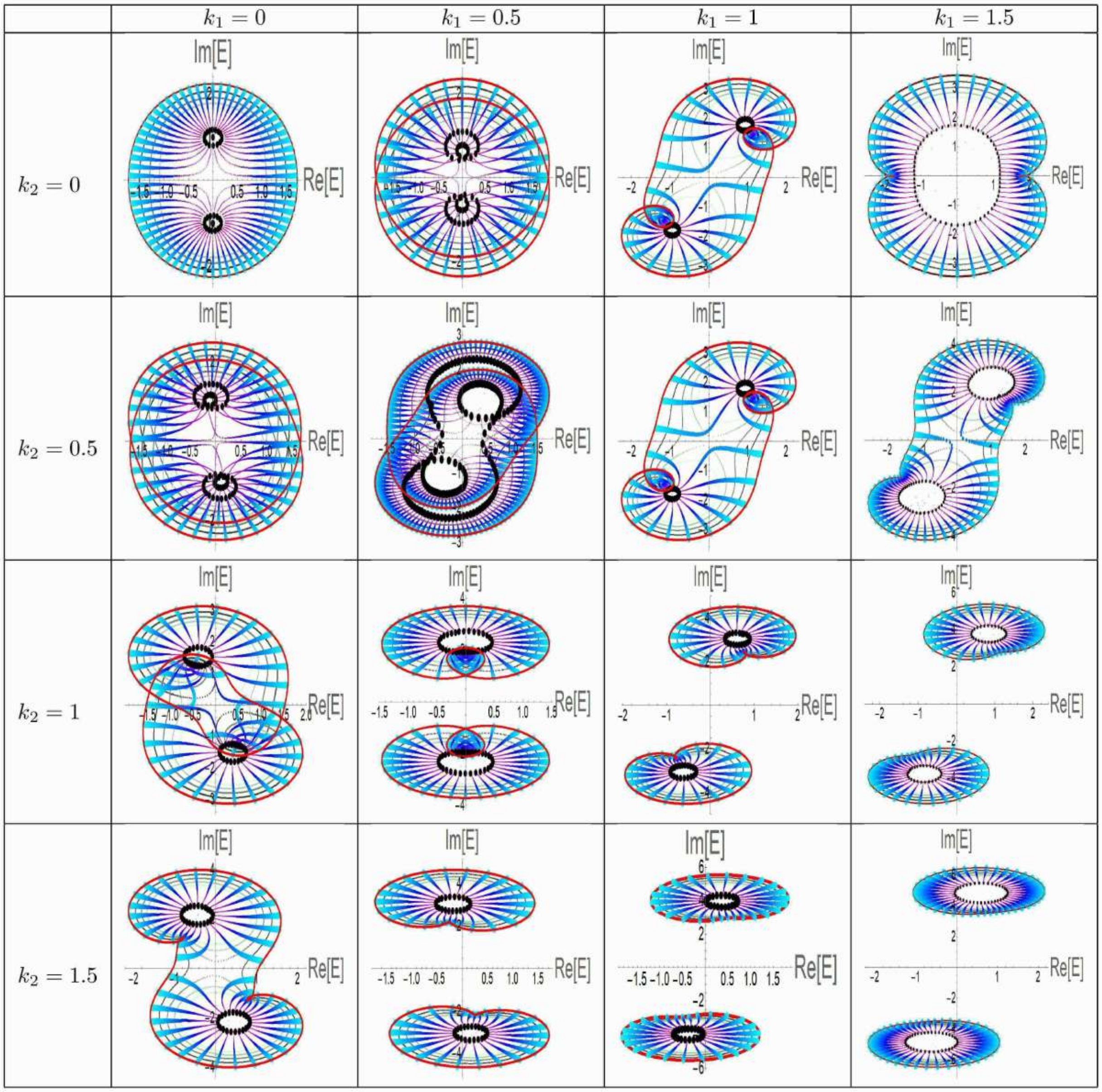

Supplemental Figure S7: Complex spectra of the non-Hermitian Trefoil nodal knot metal (NKM) with $\hat{e}_3$ surface termination. Blue-magenta curves denote the spectral flow between the spectra under periodic boundary conditions (red) and open boundary conditions (black). Background contours denote level curves of constant $\log|z|$ where $z = e^{ik_3}$. Like for the Hopf case, black loops represent the skin boundary states obtained at maximal numerical convergence.

SUPPLEMENTARY REFERENCES

* phylch@nus.edu.sg
† rthomale@physik.uni-wuerzburg.de
‡ zhangxiao@mail.sysu.edu.cn

[1] C. H. Lee and R. Thomale, Physical Review B **99**, 201103(R) (2019).